



Theoretical and Experimental Investigations of the Process of Vibration Treatment of Liquid Metals Containing Nanoparticles

S. VOROZHTSOV,^{1,2,4} O. KUDRYASHOVA,^{1,3} V. PROMAKHOV,¹
V. DAMMER,¹ and A. VOROZHTSOV^{1,3}

1.—National Research Tomsk State University, Tomsk, Russian Federation 634050. 2.—Institute of Strength Physics and Materials Science SB RAS, Tomsk, Russian Federation 634021. 3.—Institute for Problems of Chemical & Energetic Technologies SB RAS, Biysk, Russian Federation 659322. 4.—e-mail: vorn1985@gmail.com

It is known that the use of external effects, such as acoustic fields (from ultrasonic to low-frequency range), help in breaking down agglomerates, improving particle wettability, providing uniform particle distribution in the melt volume, and reducing the grain size. The fragmentation of growing crystals, de-agglomeration of particles and their mixing in liquid metal under the influence of vibration (with frequencies of 10–100 Hz) are considered in this paper. The major advantage of such a technique in comparison with high-frequency methods (sonic, ultrasonic) is the capability of processing large melt volumes proportional to the wavelength. The mechanisms of the breaking down of particle agglomerates and the mixing of particles under conditions of cavitation and turbulence during the vibration treatment of the melt are considered. Expressions linking the threshold intensity and frequency with the amplitude necessary to activate mechanisms of turbulence and cavitation were obtained. The results of vibration treatment experiments for an aluminum alloy containing diamond nanoparticles are given. This treatment makes it possible to significantly reduce the grain size and to improve the casting homogeneity and thus improve the mechanical properties of the alloy.

INTRODUCTION

Both vibration and ultrasound are reported to have a positive impact on casting quality through grain reduction, improved introduction and distribution of particles, and melt degassing.^{1,2} At the same time, the use of nanopowders in metallurgy is a very complicated issue due to the instability of nanosized substances,^{3,4} as the tendency of the particles to form agglomerates increases significantly. Some external factors have to be used to break down particle agglomerates, improve particle wetting and provide a uniform particle distribution in the melt volume. Acoustic fields (from ultrasonic to low-frequency) can be used as such external factors.

There have been many theoretical and experimental publications regarding the behavior of nanoparticles in a metallic melt in the process of their introduction, mixing and distribution in the volume upon solidification, including methods using

acoustic fields (e.g., see survey²). The mechanisms of the breaking down of nanoparticle agglomerates in metal melts under the influence of ultrasound are considered in Ref. 5. Ultrasonic treatment under the conditions of developed cavitation makes it possible to break down agglomerates and improve the wettability of the particles due to a sonocapillary effect.⁶ However, ultrasonic waves have a short wavelength, and therefore it is impossible to use them for processing large volumes of metal. Moreover, ultrasonic treatment does not provide efficient mixing of particles in the metal. Therefore, ultrasonic treatment is usually used in parallel with low-frequency (subsonic and vibration) treatment or stirring. The problem of the optimal conditions for such treatments still remains unresolved.

Many works have been dedicated to the improvement of metal microstructures by means of vibration treatment (VT),^{7–10} Many authors think that this effect can be attributed to the cavitation phenomenon or to the formation of microflows under

the influence of vibration, which breaks down growing crystals. As has been demonstrated experimentally, the grain reduction effect increases with the increase of the frequency of the vibration up to a certain value (different for different metals).⁷

It is known that to improve the physical and mechanical properties of aluminum alloys, submicron particles (including nanosized ones) of oxides, carbides and borides^{11–15} can be introduced into the melt in the process of casting. As has been shown earlier, another promising reinforcement is diamond nanoparticles (nanodiamonds).¹⁶ However, the use of such particles in metallurgy is very complicated due to their tendency to form agglomerates, and their introduction into the melt is impossible unless specific external effects are used.¹⁷ To provide an efficient distribution of reinforcing nanoparticles in the alloy and to minimize defects in the matrix structure, optimal regimes for these external effects in the process of alloy solidification need to be found. Vibration treatment has a number of advantages associated with the simplicity of the technical implementation, low energy consumption and high performance (capacity to process a large volume of the melt).

The research objective of this study is to theoretically evaluate the mechanisms of external effects in the process of the introduction of nanoparticles into a metal melt, and the breaking of agglomerates under the influence of vibration during solidification and to implement these theoretical approaches experimentally.

Mathematical Description of the Process of Vibration Treatment of Liquid Metals

The turbulent stirring of the whole mass of the melt is a top priority in the process of the low-frequency treatment of composite metallic melts. In the case of low-frequency (longwave) treatment, it is obvious that, unlike in ultrasonic treatment, the volume to be processed can be increased proportionally to the wavelength. The optimal regime will correspond to the treatment of the whole volume with the minimum intensity.

Microflows in liquid metal upon solidification affect dendrite growth and lead to grain size reduction. On the other hand, the same effect provided by cavitation in a liquid can also be realized for a liquid metal if some conditions are met. Microflows provide the uniform distribution of introduced particles in a metal volume, while cavitation causes the breakdown of agglomerates and the wetting of particles.⁵

To achieve cavitation at low frequencies, a large amplitude is required. Special conditions should be created for the formation of low pressure areas in the liquid.

The phenomenon of cavitation, when vibration affects the molten metal, was observed by Ignat'ev,¹² although he identified this phenomenon

as “pseudo-cavitation”. He emphasized that gas injection occurs when a formed cavity fills with gas from the liquid surface (melt). Under ultrasound cavitation, bubbles aggregate from the evaporation of the liquid formed in the cavity. Cavitation bubbles in the melt, both under ultrasound and vibration, behave the same way—they collapse causing a devastating shockwave.

Ignat'ev qualitatively considered the difference between the ultrasonic and vibration impacts on the melt. In particular, he writes¹² that the liquid flow under ultrasound for the half-period of oscillation is not sufficient for the creation of turbulence. Therefore, the ultrasound power is spent on the compression-tension of the melt and cavitation, while the low-frequency power is spent on turbulent mixing.¹²

Cavitation in the process of the low-frequency treatment of a liquid is a result of the displacement of volumes of the liquid along the ultrasonic wave and the formation of expansion and compression zones which cause discontinuities in the volume of the liquid. In the case of vibration treatment, such discontinuity also takes place in the liquid volume due to tensile stresses caused by the vibrations.

Thus, two phenomena in the process of low-frequency treatment may cause the breakdown of growing crystals and the introduction of nanoparticles into the melt volume: turbulent stirring and cavitation. Let us determine the critical treatment parameters corresponding to the occurrence of these phenomena.

In the framework of solving the problem of the movement of liquid microvolumes in a field of elastic vibrations, an expression for the critical frequency was obtained from Ref. 18: if the frequency of the vibrations exceeds this critical value, cavitation takes place in the melt volume,

$$f > \frac{1}{4} \sqrt{\frac{1}{A} \left(\frac{\Delta p}{2A\rho_1} - g \right)} \approx \frac{1}{A} \sqrt{\frac{\Delta p}{32\rho_1}}, \quad (1)$$

where f and A are the frequency and amplitude of the oscillations, respectively; g is the gravitational acceleration; Δp is the pressure difference; and ρ_1 is the liquid density.

Turbulence is to take place in the melt under the influence of oscillations when the Reynolds number exceeds a certain critical value,

$$Re = \frac{\rho_1 c V}{\omega b} = \frac{\rho_1 c A}{b} > Re_{cr}, \quad (2)$$

where $V = A\omega$ is the characteristic scale of the particle velocity; $\omega = 2\pi f$ is the angular frequency; c is the speed of sound; and $b = a + \nu$ is the dissipation parameter proportional to the sum of the coefficients of thermal diffusivity a and kinematic viscosity ν of the melt.

The expression for the wave field intensity links the intensity I to the frequency f and amplitude A of the oscillations:

$$A = \frac{1}{\pi f} \sqrt{\frac{I}{2c\rho_1}}. \quad (3)$$

Considering Eqs. 1 and 2, we can obtain dependences for the threshold amplitude and frequency required for the turbulence and cavitation regimes (see Fig. 1). The calculation was performed for an aluminum melt ($\rho_1 = 2357 \text{ kg/m}^3$, $c = 4700 \text{ m/s}$, $\nu = 5.0912\text{E}-7 \text{ m}^2/\text{s}$, $a = 4.082\text{E}-5 \text{ m}^2/\text{s}$ ¹⁹), and the value $Re_{cr} = 10,000$ was used as a fully developed turbulence criterion.

As follows from Eqs. 1–3, there is a minimum intensity (and an amplitude) as well as an optimal frequency sufficient to produce turbulence and cavitation regimes in the melt:

$$I_{\min} = \pi^2 \frac{\Delta p}{16} c, \quad (4)$$

$$A_{\min} = \frac{1}{\pi f} \sqrt{\frac{I_{\min}}{2c\rho_1}} = \frac{1}{f} \sqrt{\frac{\Delta p}{32\rho_1}}, \quad (5)$$

$$f_{\text{opt}} = \sqrt{\frac{\Delta p}{32\rho_1} \frac{c}{(\nu + a)Re_{cr}}}. \quad (6)$$

Two frequency ranges ($f < f_{\text{opt}}$ and $f > f_{\text{opt}}$) can be distinguished in Fig. 1. In the first, there is a large range where turbulence is possible while no cavitation occurs, while the latter requires much larger amplitudes. As the frequency grows, the cavitation regime becomes easier to achieve because the required amplitude reduces. Both mechanisms are enabled at f_{opt} , which provides the most favorable conditions for the grain size reduction and the introduction of nanoparticles into the melt. This explains an experimental fact known from the literature that, as the frequency of vibration increases (up to a certain limit)^{5,9} the casting microstructure improves.

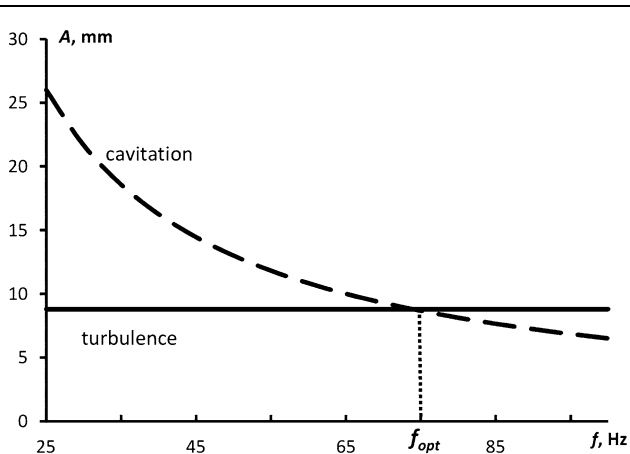


Fig. 1. Threshold frequency and amplitude of vibration: solid line turbulence threshold, dotted line cavitation threshold.

As the frequency increases, a greater intensity is required to maintain the target amplitude according to Eq. 3, but this is not always possible for the devices used. Therefore, the actual amplitude decreases and becomes insufficient to maintain efficient turbulence and cavitation regimes, which results in the reduction of the effects.

As follows from Eqs. 5 and 6, the required amplitude and frequency of the vibration treatment depend significantly on the metal's properties: speed of sound, density, viscosity and thermal diffusivity. Therefore, these parameters will be different for different metals and alloys. The values of the optimal frequency of vibration treatment calculated for various metals (according to the physical data from Ref. 19) are shown in Fig. 2. The calculation of the minimum required amplitude of the vibration treatment is shown in Fig. 3. The optimal frequency for aluminum is, therefore, 75 Hz, and the minimum amplitude is 8 mm.

The turbulence and cavitation generated by the vibration device may break down growing metal crystals and particle agglomerates. An excess pressure near the agglomerate pores is created in the process of the collapse of cavitation bubbles. This pressure enables the impregnation of the agglomerate pores and their further breakdown, as described in detail in Ref. 5. Microflows generated by the vibration also provide the mixing of the particles in the melt. Let us move to a more detailed consideration of this issue.

Acoustic flows provide the mixing of particles in the melt volume. In the case of low-frequency oscillations, we can consider small-scale flows with a characteristic vortex size on the order of the acoustic boundary layer:¹¹

$$\delta_a = \sqrt{\frac{2\nu}{\omega}} = \sqrt{\frac{\nu}{\pi f}}. \quad (7)$$

The size of this boundary layer for an aluminum melt and a frequency of 50 Hz is approximately 0.2 mm (see Table I). Such small vortices, however,

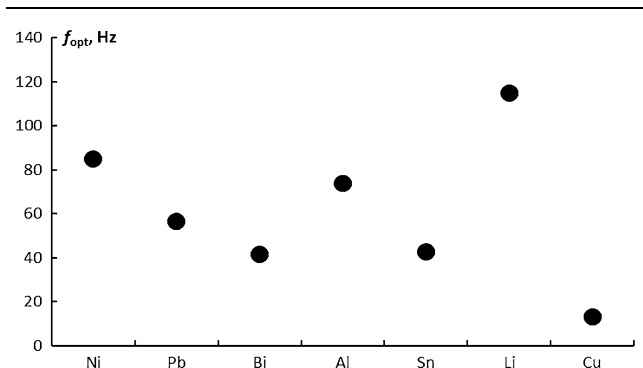


Fig. 2. Optimal frequency of vibration treatment for various metal melts.

are significantly larger than the particles (or even agglomerates), and thus they will provide their mixing.

Thus, the results of the theoretical studies presented here provide a basis for the selection of the optimal parameters of the external action on a metallic melt in the process of nanoparticle introduction to provide their experimental verification.

EXPERIMENTAL

Production of Aluminum Alloy with Nanodiamonds Under Vibration Treatment

As was shown earlier,^{16,20} aluminum alloys reinforced with diamond nanoparticles demonstrate high performance and mechanical properties. Therefore, particles were introduced into the melt of a commercial A356 aluminum alloy of the Al–Si system using a prepared master alloy and vibration treatment. The master alloy (Al + 10 wt.% nanodiamonds) in the form of a rod (up to 1 m in length) was synthesized by the shock-wave compaction method described in detail in Ref. 17.

An experimental assembly for the vibration treatment of metallic melts is shown in Fig. 4. The control of the frequency of the vibration treatment is carried out using a frequency analyzer. At the first stage, a master alloy with nanoparticles was introduced into the liquid metal at a constant melt temperature of 720°C. As soon as the master alloy is dissolved in the crucible, intensive mechanical stirring is performed for 2 min. The impeller was made from Ti alloy and coated with a high-temperature ceramic glue to minimize Ti pick up in the aluminum during stirring processing. Then, the liquid alloy was poured at 700°C into a metallic mold with a cavity size of diameter 35 × 120 mm. The nominal nanoparticle content in the alloy was 0.5 wt.%. Two reference samples (one without nanoparticle introduction and without vibration treatment and the other without nanoparticles but with vibration treatment) were made to study the influence of the nanoparticles and vibrations on the properties of the melted materials.

Then, the melt was poured into a mould (preheated at 150°C to ensure minimum porosity in the casting) with simultaneous air cooling and vibration treatment.

The parameters of the vibration treatment of the aluminum melt used in the experiment, selected on the basis of theoretical studies (Eqs. 5 and 6), are given in Table II.

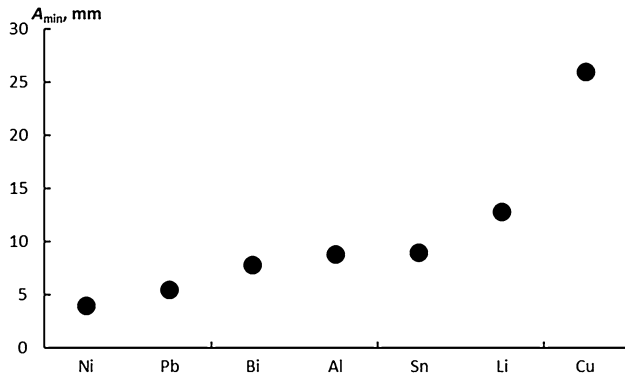


Fig. 3. Minimum amplitude of vibration treatment for different metals.

Table II. Parameters of vibration treatment of aluminum melt

Amplitude (mm)	Frequency (Hz)
8	75

Table I. Scale of microflows in the melt depending on treatment frequency (calculated for aluminum)

f (Hz)	5	10	15	20	25	30	35	40	45	50	55	60	75
δ (mm)	0.57	0.40	0.33	0.28	0.25	0.23	0.22	0.20	0.19	0.18	0.17	0.16	0.15

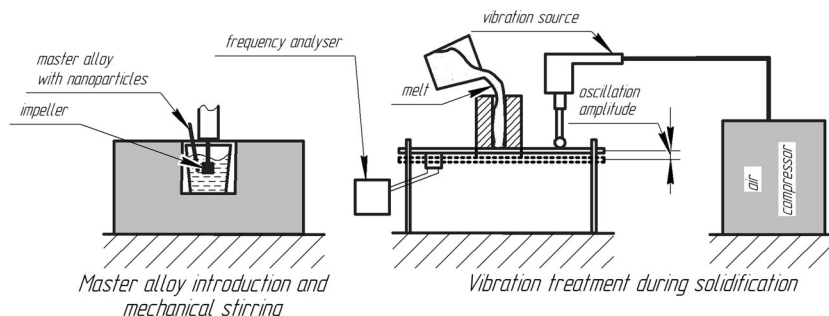


Fig. 4. Experimental assembly for vibration treatment of metal melts.

Methods of Structure and Property Investigation

The test materials were samples from (1) a commercial A356 aluminum alloy in the as-cast state, (2) A356 + VT and (3) A356 + 0.5 wt.% of nanodiamonds + VT.

The samples for the microstructural studies were taken from different sections of the casting (edge and core). Longitudinal sections of the samples were prepared for a macrostructural study. Macro-etching of the aluminum alloys was performed by dipping samples into a solution of 5% HF, 25% HNO₃, and 70% HCl.

The polished alloy surface was anodized to study the microstructure of the obtained alloys. This procedure was performed using a 5% HBF₄ solution as an electrolyte at a voltage of ~ 20 VDC.

Flat tensile samples 1 mm thick with a gauge length of 40 mm were cut from the cylindrical castings and tested in an Instron 3369 tensile machine (Instron, USA) at a strain rate of $2 \times 10^{-4} \text{ s}^{-1}$. The guaranteed frame stiffness for this machine corresponds to a 250-kN load and a load accuracy of 0.5% of the indicated load. The ultimate load during the sample testing procedures did not exceed 1.5 kN.

EXPERIMENTAL RESULTS AND DISCUSSION

An experimental study of the influence of the vibration treatment of the melt at a selected optimal vibration frequency was carried out. The treatment

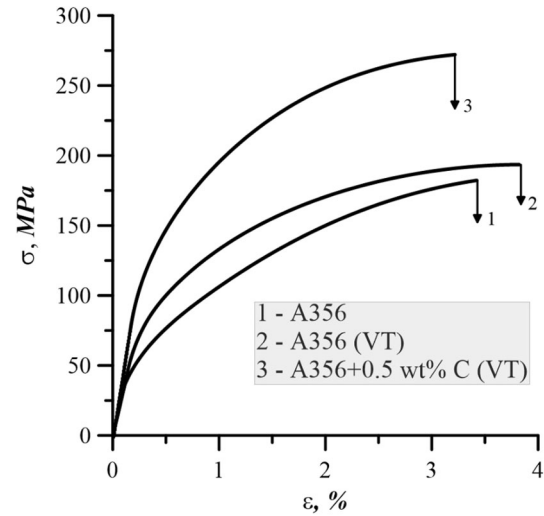


Fig. 6. Stress–strain diagrams of an aluminum alloy A356.

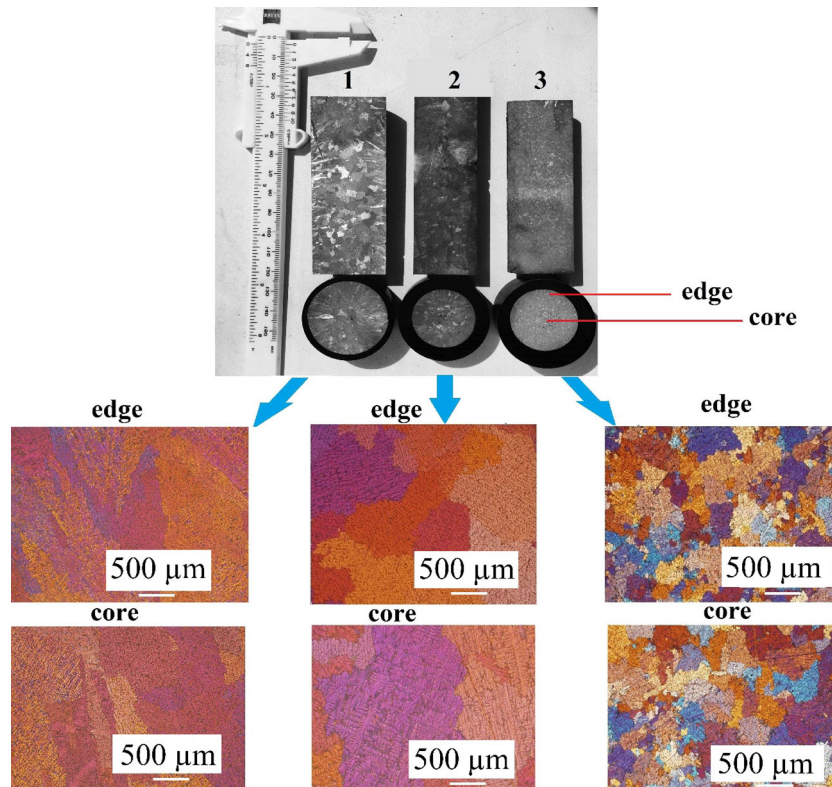


Fig. 5. Macro- and microstructure of A356 samples produced under different conditions: 1 plain casting; 2 vibration; and 3 vibration and nanodiamond addition.

Table III. Mechanical properties of alloys obtained using vibration treatment

Alloy	Yield strength (MPa)	Ultimate tensile strength (MPa)	Elongation (%)
A356	48 ± 5	168 ± 7	3.4 ± 0.2
A356 (VT)	60 ± 5	185 ± 12	3.8 ± 0.2
A356 + 0.5% wt.% C (VT)	91 ± 10	272 ± 12	3.2 ± 0.3

was performed during alloy solidification. Due to the vibrations, two-phase liquidus–solidus areas are fragmented, and the length of the capillary is reduced. Reducing the capillary length leads to an increase in the flow rate of liquid alloy within and to the “improvement” of the conditions of filling micro-heterogeneities. As a result, the average grain size decreases.

The nanodiamonds used as reinforcement particles in alloy production are described in detail elsewhere.²¹ The powder has a fine morphology with an average particle size of 4 nm and also contains particle agglomerates with a size up to 10 μm. The x-ray phase analysis revealed that the nanodiamond powder contains ~40% of the x-ray amorphous carbon phase and ~45% of the diamond phase, while the rest is crystalline carbon.

The macro- and microstructure of the aluminum alloy obtained using vibration treatment is presented in Fig. 5. It can be observed that the solidification of the initial alloy A356 results in the formation of coarse columnar grains (especially near the walls of the mold). The grain morphology in the interior of the casting is irregular, with coarse (0.5–2 mm) grains. The vibration treatment of the melt during the solidification of the A356 alloy leads to a more uniform grain morphology, close to the equiaxed. This may be the result of grain fragmentation and a more uniform temperature distribution in the melt due to melt agitation (hence, a smaller thermal gradient). However, the average grain size at the edge of the casting is almost 2 times smaller (0.8 mm) than that at the core of the sample (1.5 mm). The introduction of 0.5 wt.% nanodiamonds and melt solidification with simultaneous vibration treatment significantly affects the grain structure. In this case, the casting structure is much more uniform, and the grain size does not change from the core to the edge of the sample, remaining approximately 0.5 mm on average (see Fig. 5). Thus, in the process of melt solidification, nanoparticles may play a role of the solidification of nuclei. In addition, agglomerates of nanoparticles are pushed to the grain boundaries, which is an additional factor in the grain growth restriction.

A series of stress–strain diagrams of the A356 aluminum alloy are shown in Fig. 6. It can be observed that the vibration treatment of the A356 alloy leads to an improvement in the tensile properties, and the introduction of nanoparticles into the A356 alloy and thus the alloy reinforcement and

grain refinement leads to significant improvements in the mechanical properties (ultimate tensile strength, yield strength, Young’s modulus and hardness) without a ductility reduction. Two strengthening mechanisms (Hall–Petch and Orowan strengthening) can make contributions to the improvement of the mechanical properties in this case. The values of the mechanical properties of the obtained alloys are given in Table III.

SUMMARY

The mechanisms of the breakdown of growing crystals and particle agglomerates in the melt during the low-frequency vibration treatment of a solidifying alloy (turbulence and cavitation) were studied and analyzed. Expressions for the turbulence and cavitation thresholds for the low-frequency treatment were obtained. It was found that there is an optimal vibration frequency providing the combination of cavitation and turbulence that may lead to the formation of a better structure. The explanation of this phenomenon is given along with obtained expressions that determine this frequency as well as the required amplitude. These values are calculated for various metals. Thus, the optimal frequency for the aluminum melt is 75 Hz, with a minimum amplitude of 8 mm.

According to the theoretical calculations and experimental data, the use of a vibration treatment (with optimal parameters) leads to the optimization of the grain morphology of an aluminum alloy. At the same time, the introduction of diamond nanoparticles with simultaneous vibration treatment significantly reduces the grain size of the alloy and leads to a significant improvement of the mechanical properties of the alloys compared to those of a reference alloy.

ACKNOWLEDGEMENTS

The work was financially supported by the Ministry of Education and Science of the Russian Federation within the framework of the Federal Target Program. Agreement No. 14.578.21.0098 (Unique identifier RFMEFI57814X0098).

REFERENCES

1. C. Vives, *JOM* 50, 1 (1998).
2. G.I. Eskin and D.G. Eskin, *Ultrasonic Treatment Light Alloy Melts* (London: CRC Press, 2014), p. 346.
3. M.A. Korchagin and D.V. Dudina, *Comb. Expl. Shock Waves* 43, 176 (2007).

4. M. Lerner, A. Vorozhtsov, S. Guseinov, and P. Storozhenko, *Metal Nanopowders: Production, Characterization, and Energetic Applications*, ed. A. Gromov and U. Teipel (New York: Wiley-VCH Verlag GmbH & Co. KGaA, 2014), p. 79.
5. O. Kudryashova and S. Vorozhtsov, *JOM* 68, 1307 (2016).
6. M. Estruga, L. Chen, H. Choi, X. Li, and S. Jin, *A.C.S. Appl. Mater. Interfaces* 5, 8813 (2013).
7. W. Jiang, X. Chen, B. Wang, Z. Fan, and H. Wu, *Int. J. Adv. Manuf. Technol.* 83, 167 (2016).
8. F. Taghavi, H. Saghafian, and Y. Kharrazi, *Mater. Des.* 30, 1604 (2009).
9. G. Chirita, I. Stefanescu, D. Soares, and F.S. Silva, *Mater. Des.* 30, 1575 (2009).
10. A.F. Olufemi and I.S. Ademola, *Int. J. Metall. Eng* 1, 40 (2012).
11. S. Vorozhtsov, I. Zhukov, A. Vorozhtsov, A. Zhukov, D. Eskin, and A. Kvetinskaya, *Adv. Mater. Sci. Eng* 2015, 1 (2015).
12. I.E. Ignat'ev, E.A. Pastukhov, and E.V. Ignat'eva, *Russ. J. Non-Ferr. Met.*, 6, 509 (2014).
13. A.D. Moghadam, B.F. Schultz, J.B. Ferguson, E. Omrani, P.K. Rohatgi, and N. Gupta, *JOM* 66, 872 (2014).
14. D. Stefanescu, B. Dhindaw, S. Kacar, and A. Moitra, *Metal. Trans. A* 19, 2847 (1988).
15. S. Vorozhtsov, V. Kolarik, V. Promakhov, I. Zhukov, A. Vorozhtsov, and V. Kuchenreuther-Hummel, *JOM* 68, 1312 (2016).
16. S.A. Vorozhtsov, A.P. Khrustalyov, D.G. Eskin, S.N. Kulkov, and N. Alba-Baena, *Russ. Phys. J.* 57, 1485 (2015).
17. S.A. Vorozhtsov, D.G. Eskin, J. Tamayo, A.B. Vorozhtsov, V.V. Promakhov, A.A. Averin, and A.P. Khrustalyov, *Metal. Trans. A* 46A, 2870 (2015).
18. I.E. Ignat'ev, A.V. Dolmatov, E.V. Ignat'ev, S.A. Istomin, and E.A. Pastukhov, *Russ. Metall. (Metally)* 12, 97 (2012).
19. I.S. Grigoryeva and E.Z. Meylikhova, eds., *Physical Properties* (Moscow: Energoatomizdat, 1981), p. 1232.
20. S. Vorozhtsov, D. Eskin, A. Vorozhtsov, and S. Kulkov, *Light Metals 2014* (Warrendale: TMS, 2014), p. 1373.
21. A.A. Gromov, S.A. Vorozhtsov, V.F. Komarov, G.V. Sakovich, Y.I. Pautova, and M. Offermann, *Mater. Lett.* 91, 198 (2013).